43rd AIAA Aerospace Sciences Meeting and Exhibit
10-13 January 2005, Reno, Nevada

AIAA 2005-831

Sensitivity Enhancement in Laser Absorption Spectroscopy for the Diagnostics of High-Enthalpy Flows

Hiroki Takayanagi,* Makoto Matsui,† Kimiya Komurasaki,‡ and Yoshihiro Arakawa§
The University of Tokyo, Tokyo, 113-8656, Japan

In absorption spectroscopy of high enthalpy flows generated by plasma wind tunnels, number density of meta-stable OI tends to be too small to be detected. In this study, a new multipass method is proposed for sensitivity enhancement in laser absorption spectroscopy, in which test plasma is placed between a diode laser and a diffraction grating of an external cavity diode laser. As a result, frequency could be tuned continuously by the ECDL with long cavity length and absorption is observed with the multipass optics.

Nomenclature

A	=	Einstein coefficient
B	=	bimolecular recombination coefficent
c	=	velocity of light
E	=	energy gap
E_{os}	=	stored optical energy in the cavity
g	=	statistical weight
h	=	Planck's constant
i	=	absorbing state
j	=	excited state
I_0	=	optical power output of laser without plasma
I_{inj}	=	injection current
I_t	=	optical power output of laser with plasma
I_{th}	=	threshold current
I_{th0}	=	threshold current without plasma between diode laser and diffraction grating
I_{thp}	=	threshold current with plasma between diode laser and diffraction grating
ΔI	=	decreasing of the optical power output by plasma absorption
$\Delta I/I_0$	=	absorbance
$(\Delta I/I_0)_{IN}$	=	absorbance with plasma in external cavity diode laser
$(\Delta I/I_0)_{OUT}$	=	absorbance with plasma out of external cavity diode laser
k	=	Boltzmann constant
K	=	integrated absorption coefficient
k_ν	=	absorption coefficient
L_{ext}	=	external cavity length
ΔL_{ext}	=	deflection of external cavity length
L_{int}	=	active region length of diode laser
m	=	integer
M_A	=	atomic mass
N_i	=	number density of absorbing state
N_p	=	photon density
N_{tr}	=	transparency carrier density
q	=	elementary charge

* Graduate student, Department of Aeronautics and Astronautics, takayanagi@al.t.u-tokyo.ac.jp, and Student Member AIAA
† Graduate student, Department of Advanced Energy, matsui@al.t.u-tokyo.ac.jp, and Student Member AIAA
‡ Assosiate Proffessor, Department of Advanced Energy, komurasaki@k.u-tokyo.ac.jp, and Senior Member AIAA
§ Professor, Department of Aeronautics and Astronautics, arakawa@al.t.u-tokyo.ac.jp, and Senior Member AIAA

r_{eff} = effective reflection coefficient of the external cavity
r_{f1} = reflection coefficient of the high-reflection-coated facet
r_{f2} = reflection coefficient of the anti-reflection-coated facet
r_g = reflection coefficient of the diffraction grating
T = Temperature
V = active region volume occupied by electrons
V_p = cavity volume
v_g = group velocity
x = coordinate in laser pass
$<\alpha_0>$ = sum of averaged internal loss and mirror loss
$<\alpha_i>$ = averaged internal loss
α_m = mirror loss
$<\alpha_p>$ = average plasma loss
$\tilde{\beta}_{ext}$ = wave number of laser
η_i = internal quantum efficiency
λ = wavelength of laser
λ_0 = center absorption wavelength
ν = laser frequency
ν_0 = center absorption frequency
$\Delta\nu$ = width of laser frequency modulation
$\Delta\nu_D$ = full width at half maximum

I. Introduction

In past five decades, high enthalpy flow generators have been developed to simulate re-entry conditions.[1] However, their exact plume conditions are mostly unknown because they are usually in strong thermo-chemical non-equilibrium.

In our previous study, Laser Absorption Spectroscopy (LAS) was applied to plumes of arc-heaters and an Inductive Plasma Generator[2,3] (IPG) to measure the number density of meta-stable OI and translational temperature. As a result, strong absorption lines of OI 777.19nm line were observed in oxygen and argon/oxygen flows for these high enthalpy flow generators. However, OI absorption could not be detected in a nitrogen/oxygen flow even in a shock layer formed in front of test materials as well as free stream. The absorbance would be less than our measurement limit of 1%.

In this research, number density of meta-stable OI and temperature for given specific enthalpy are estimated for pure oxygen, argon/oxygen, and nitrogen/oxygen flows. Next, the threshold density of meta-stable OI for LAS is estimated. Finally a new multipass method for sensitivity enhancement is proposed and tested.

II. Applicable Limit of LAS in High Enthalpy Flows

A. Previous results in IPG

Figure 1 shows absorbance, $(I_0\text{-}I_t)/I_0$, in pure oxygen and nitrogen/oxygen flows generated by IPG at the University of Stuttgart[4]. The absorbance in a nitrogen/oxygen flow was much lower than that in an oxygen flow. In arc-heaters plumes, absorption couldn't be detected in nitrogen/oxygen flows though 50% absorbance was observed in argon/oxygen flows.

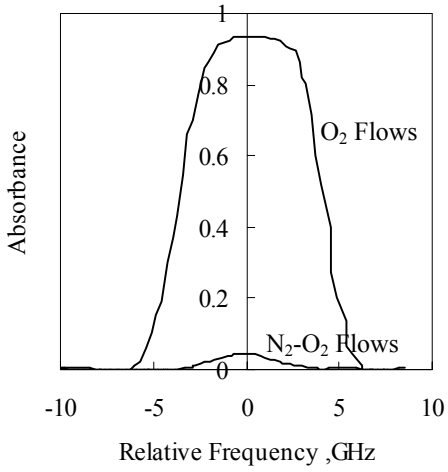

Figure 1 Absorbance in pure oxygen (3g/110kW) and nitrogen/ oxygen flows (3g/130kW).

B. Calculation under Thermo-chemical Equilibrium

The lower absorption in nitrogen/oxygen flows is explained by the calculation under thermo-

chemical equilibrium. Temperature was calculated for oxygen, argon/oxygen, and nitrogen/oxygen flows as a function of specific total enthalpy at the ambient pressure of 30Pa, as shown in Fig. 3. Oxygen is dissociated around 2,500K while nitrogen is around 5000K. Then temperature in nitrogen/oxygen flows hardly increases at all. As a result, assuming the Boltzmann equilibrium, the number density of meta-stable OI in nitrogen/oxygen flows is about two orders of magnitude smaller than that in argon/oxygen and pure oxygen flows as shown in Fig. 4 in the enthalpy range of the IPG. Actual number density of meta-stable OI is usually higher than estimated because of the decaying non-equilibrium in expanding high enthalpy flows. The maximum number density of meta-stable OI in pure oxygen was measured about 3.5×10^{17}m^{-3}. So that in nitrogen/oxygen flows would be 1×10^{14}m^{-3}.

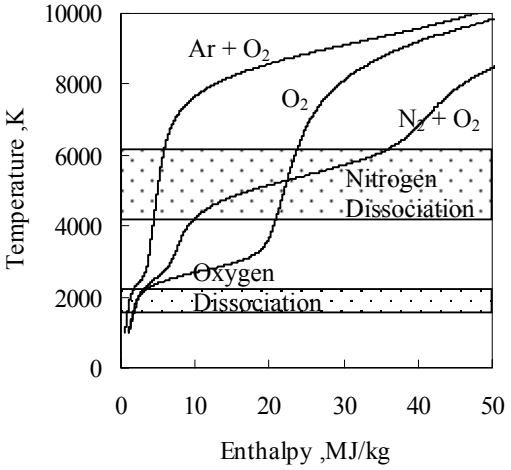

Figure 3. Calculated Temperature vs Specific Total Enthalpy. *p* = 30[Pa].

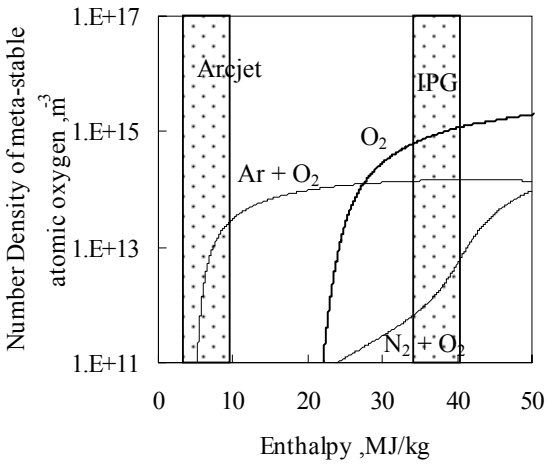

Figure 4. Number Density of meta-stable OI vs Specific Total Enthalpy. *p* = 30[Pa].

C. Lower Limit Number Density of Meta-stable OI

The relationship between laser intensity and absorption coefficient is expressed by the Beer-Lambert law[5] as,

$$\ln\frac{I_t}{I_0} = -\int k_\nu(x)\,dx\,. \tag{1}$$

Assuming Boltzmann equilibrium between the absorbing and excited states, the integrated absorption coefficient K is proportional to the number density at the absorbing state N_i as,

$$K \equiv \int_{-\infty}^{\infty} k_\nu d\nu = \frac{\lambda_0^{\,2}}{8\pi}\frac{g_j}{g_i}A_{ji}N_i\left[1-\exp\left(-\frac{\Delta E_{ij}}{kT_{\mathrm{ex}}}\right)\right]. \tag{2}$$

Transition data of target absorption lines in this study are listed in Table 1. $\Delta E_{ij}/kT_{\mathrm{ex}}$ is so large that Eq. (2) is approximated as

$$K = \frac{\lambda_0^{\,2}}{8\pi}\frac{g_j}{g_i}A_{ij}N_i\,. \tag{3}$$

Since the Doppler broadening is predominant in our test conditions, absorption profile is expressed by the Gaussian one as,

$$k_\nu = k_{\nu_0}\cdot\exp\left[-\left(\frac{\nu_0-\nu}{\Delta\nu_{\mathrm{D}}/2\sqrt{\ln 2}}\right)^2\right]. \tag{4}$$

Then, K is expressed as,

$$K = k_{\mathrm{r}}(\nu_0)\sqrt{\pi}\,\frac{\Delta\nu_{\mathrm{D}}}{2\sqrt{\ln 2}}\,. \tag{5}$$

Here, $\Delta\nu_{\mathrm{D}}$ is related to T as

$$\Delta\nu_{\mathrm{D}} = \frac{2\nu_0\sqrt{\ln 2}}{c}\sqrt{\frac{2kT}{M_{\mathrm{A}}}}\,. \tag{6}$$

Table 1 Translation data

Parameters	Species	
	OI	ArI
I	$3s^5S$	$4s^{2[1/2]}$
j	$3p^5P$	$4s^{2[3/2]}$
λ ,nm	777.19	840.82
E_i ,eV	9.14	11.8
E_j ,eV	10.7	13.3
g_i	5	3
g_j	7	5
A_{ji} ,10^8s^{-1}	0.369	0.223

Assuming T, the relationship between absorbance and number density of meta-stable OI is calculated using Eqs. (1,3-5). Figure 2 shows the relationship between absorbance and number density at T=3000±2000K. Here, error bar corresponds to the temperature variation. When detectable absorbance is about 0.01, the limit number density of meta-stable OI is about 1×10^{15}[m^{-3}].

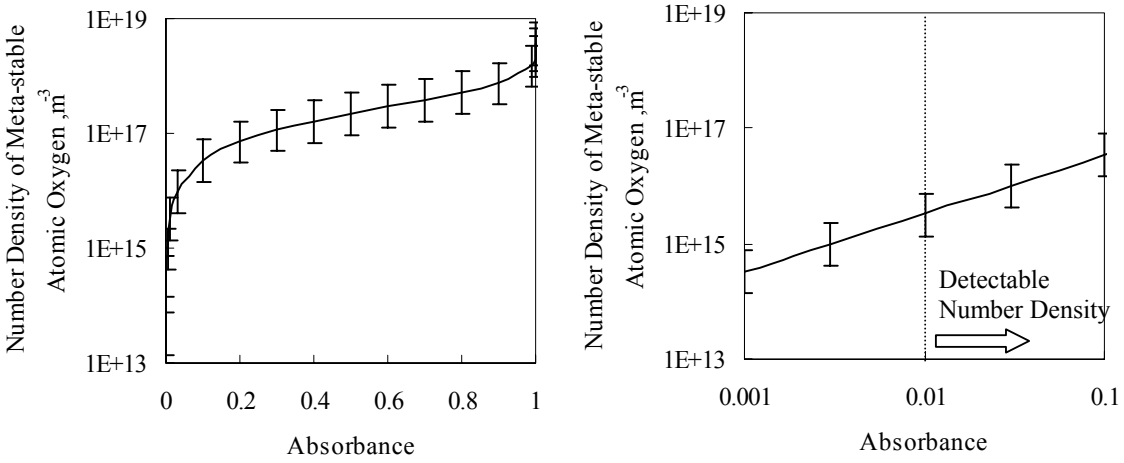

Figure 2 Relationship between absorbance and number density of meta-stable OI. Left is plotted for overall range of absorbance and right is plotted in log-scale.

III. A New Multipass Method of Sensitivity Enhancement using ECDL

A. Concept of a new multipass method

Equation (1) indicates that the sensitivity of absorbance is exponentially increases with the absorption path length. Therefore, multipass absorption cells[6,7] are conventionally used to enhancement the sensitivity in laser absorption spectroscopy. However, the spatial resolution is sacrificed in this method, and then it is not effective for the measurement of high enthalpy flows because the plumes vary spatial variation of physical properties is inevitable and very important.

Therefore, a new multipass method is proposed. Test plasma is placed between a diode laser and a diffraction grating of External Cavity Diode Laser (ECDL) as shown schematically in Fig. 5. The cavity is formed between high-reflection coated facet of a diode laser and a diffraction grating. The laser wavelength is specified in this cavity. The wavelength can be tuned by modulating the cavity geometry. If there is somewhat laser absorption in the plasma, the output intensity would decrease due to the absorption of plasma. Because multi-laser-pass is realized in this cavity, absorbance would be magnified depending on the effective number of passes.

B. Analytical Simulation[8]

By the equations for diode laser, analytical simulation for the proposed method is calculated. To obtain the optical power output, E_{os} is constructed by multiplying N_p by $h\nu$, and V_p. Then, this is multiplied by the energy loss rate through the mirrors, $v_g\alpha_m$, to get optical power output from the mirrors,

$$I_0 = v_g \alpha_m E_{OS} = v_g \alpha_m N_p h\nu V_p \qquad (7)$$

Here v_g is the group velocity, and α_m is the mirror loss given by

$$\alpha_m = \frac{1}{L_{int}} \ln\left(\frac{1}{r_{fl} r_{eff}(\nu)}\right). \qquad (8)$$

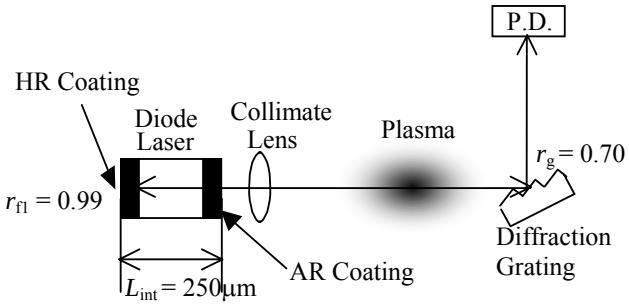

Figure. 5 Schematic of Sensitivity Enhancement

where r_{eff} is given by

$$r_{\mathrm{eff}}(\nu) = r_{\mathrm{f2}} + \frac{(1-r_{\mathrm{f2}})^2 r_{\mathrm{ext}} \exp\left(-2j\tilde{\beta}_{\mathrm{ext}} L_{\mathrm{ext}}\right)}{1 + r_{\mathrm{f2}} r_{\mathrm{ext}} \exp\left(-2j\tilde{\beta}_{\mathrm{ext}} L_{\mathrm{ext}}\right)}. \tag{9}$$

From carrier rate equation, the photon density is obtained as following equation.

$$N_{\mathrm{p}} = \frac{\eta_i \left(I_{\mathrm{inj}} - I_{\mathrm{th}}\right)}{q v_{\mathrm{g}} g_{\mathrm{th}} V} \tag{10}$$

From photon generation and loss in laser cavity, the following equation is obtained.

$$\Gamma g_{\mathrm{th}} = \langle \alpha_{\mathrm{i}} \rangle + \alpha_{\mathrm{m}}. \tag{11}$$

Substituting Eqs. (8) and (10) to Eq. (7), the following equation is obtained.

$$I_0 = \eta_{\mathrm{i}} \left(\frac{\alpha_{\mathrm{m}}}{\langle \alpha_{\mathrm{i}} \rangle + \alpha_{\mathrm{m}}} \right) \frac{h\nu}{q} \left(I_{\mathrm{inj}} - I_{\mathrm{th}}\right) \tag{12}$$

I_{th} is expressed as

$$I_{\mathrm{th}} \approx \frac{qVBN_{\mathrm{tr}}^{\ 2}}{\eta_{\mathrm{i}}} \exp\left\{ \frac{2\left(\langle \alpha_{\mathrm{i}} \rangle + \alpha_{\mathrm{m}}\right)}{\Gamma g_0} \right\}. \tag{13}$$

Using a constant γ, threshold injection current is rewritten as follows.

$$I_{\mathrm{th}} \approx \gamma \exp\left\{ \frac{2\left(\langle \alpha_{\mathrm{i}} \rangle + \alpha_{\mathrm{m}}\right)}{\Gamma g_0} \right\} \tag{14}$$

When plasma is placed in between a diode laser and a diffraction grating, loss due to the plasma absorption

$$\langle \alpha_{\mathrm{p}} \rangle \equiv \frac{\int k_{\mathrm{v}}(x)\, dx}{L_{\mathrm{int}}} \tag{15}$$

is added to $<\alpha_{\mathrm{i}}>$. Then, Eqs. (12) and (14) is rewritten as follows.

$$I_{\mathrm{t}} = \eta_{\mathrm{i}} \left(\frac{\alpha_{\mathrm{m}}}{\alpha_0 + \langle \alpha_{\mathrm{p}} \rangle} \right) \frac{h\nu}{q} \left(I_{\mathrm{inj}} - I_{\mathrm{thp}}\right) \tag{16}$$

$$I_{\mathrm{thp}} \approx \gamma \exp\left\{ \frac{2\left(\alpha_0 + \langle \alpha_{\mathrm{p}} \rangle\right)}{\Gamma g_0} \right\} = I_{\mathrm{th0}} \exp\left(\frac{2\langle \alpha_{\mathrm{p}} \rangle}{\Gamma g_0} \right). \tag{17}$$

From Eq.(12) and (16), the absorbance with plasma in ECDL is obtained as

$$\left(\frac{\Delta I}{I_0} \right)_{\mathrm{IN}} = 1 - \frac{I_{\mathrm{t}}}{I_0} = 1 - \frac{1}{1 + \langle \alpha_{\mathrm{p}} \rangle / \alpha_0} \frac{I_{\mathrm{inj}} - I_{\mathrm{th0}} \exp\left(2\langle \alpha_{\mathrm{p}} \rangle / \Gamma g_0\right)}{I_{\mathrm{inj}} - I_{\mathrm{th0}}} \tag{18}$$

where I_{th0} is the threshold current with plasma out of ECDL calculated by Eq. (14). Here the absorbance with plasma out of ECDL is defined as $(\Delta I/I_0)_{\mathrm{OUT}}$. Then, Eq. (15) is rewritten as

$$\langle \alpha_{\mathrm{p}} \rangle = \frac{-\ln\left\{1 - (\Delta I/I_0)_{\mathrm{IN}}\right\}}{\mathrm{L}_{\mathrm{int}}} \tag{19}$$

When plasma is placed in ECDL, the threshold current increases and the gradient of optical power output is lower as shown in Fig. 6.

In Fig. 7, the output power characteristics are plotted for various absorbance using the parameters common to in-plane lasers listed in Table 2. In diode laser with an Anti-Reflection coating on one facet and High-Reflection coating for the other facet, r_{f2} is assumed 0 and r_{eff} is equal to r_{g}. r_{f1} and r_{g} are approximated at 0.99 and 0.70, respectively. Then, α_{m} is estimated at 15cm^{-1}.

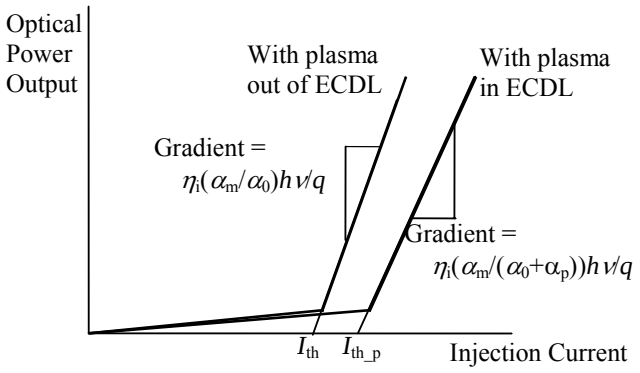

Figure 6 Schematic of output power vs. injection current.

$(\Delta I/I_0)_{IN}$ is plotted in Fig. 8. When the injection current approaches to the threshold, $(\Delta I/I_0)_{IN}$ would be larger. Figure 9 shows the simulated absorption profiles. $(\Delta I/I_0)_{OUT}$ is the experimental result in the nitrogen/oxygen plume as shown in Fig. 1. The rate of $(\Delta I/I_0)_{IN}$ to $(\Delta I/I_0)_{OUT}$ is larger when $(\Delta I/I_0)_{OUT}$ is large. Then, The rates of $(\Delta I/I_0)_{IN}$ to $(\Delta I/I_0)_{OUT}$ are different for the frequency in the absorption profile. The broadening width changes with the injection current. Therefore, to have true broadening width and absorption coefficient, profiles have to be fitted to Eqs. (18) and (19).

Table 2 List of Common Parameters for In-Plane Laser

parameters	Values
V	$4\times10^{-6}\mathrm{m}^3$
Γg_0	57.6 cm^{-1}
α_i	$5\mathrm{cm}^{-1}$
η_i	0.8
N_{tr}	$1.8\times10^{24}\mathrm{m}^{-3}$
B	$7.38\times10^{-11}\mathrm{cm}^3/\mathrm{s}$
I_{th0}	0.38mA

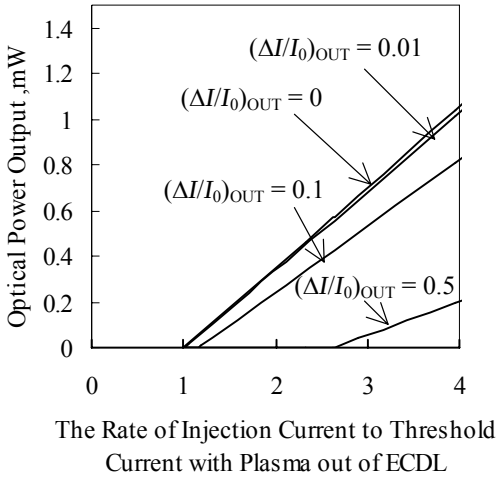

Figure 7. Power Output characteristics for various absorbance.

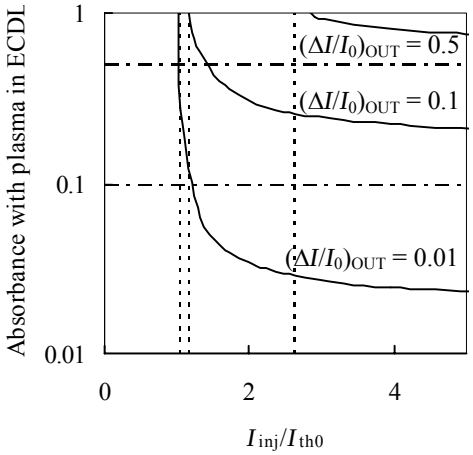

Figure 8 I_{inj} vs. absorbance. Dotted lines are I_{th0} for respective absorbance.

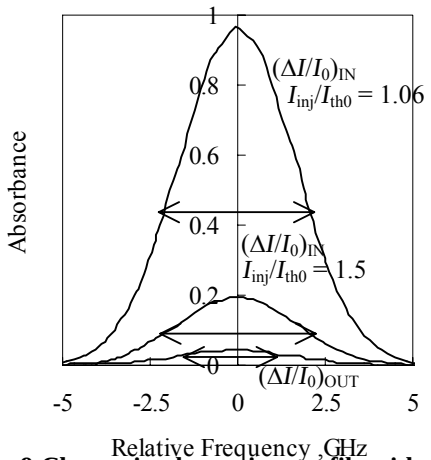

Figure 9 Change in absorption profile with the injection current between $(\Delta I/I_0)_{OUT}$ and $(\Delta I/I_0)_{IN}$.

IV. Experiment by ECDL with long cavity length

A. Experimental Apparatus

ECDL is commercially available. However, in these ECDLs, the cavity length is so short, that plasma cannot be placed in ECDL. Therefore, ECDL with long cavity length was developed. For the validation of the proposed method, the argon glow discharge tube was used, where length is 10cm. So the cavity length is 30cm. From resonance condition, a following equation is obtained[9],

$$\Delta L_{\text{ext}} = \frac{\Delta \nu}{\nu} L_{\text{ext}} \,. \tag{20}$$

In Fig.10, the relationship between ΔL_{ext} and L_{ext} is shown when width of laser frequency modulation $\Delta \nu$ is 3.0GHz.

Measurement system is shown in Fig. 11. The AR coated diode laser made by Sacher Lasertechnik and the diffraction grating made by Edmund Optics Co. are used. Here Littrow configuration is adopted for easy alignment. The beam is collimated. The cavity length is tuned continuously by the piezo actuator. The temperature of the diode laser is adjusted by the temperature controller with the peltier device. Isolator eliminate feedback. The time is translated into the frequency using etalon. The optical power output is measured by the photo detector. Replacing the glow discharge tube, $(I_t/I_0)_{\text{OUT}}$ and $(I_t/I_0)_{\text{IN}}$ are measured.

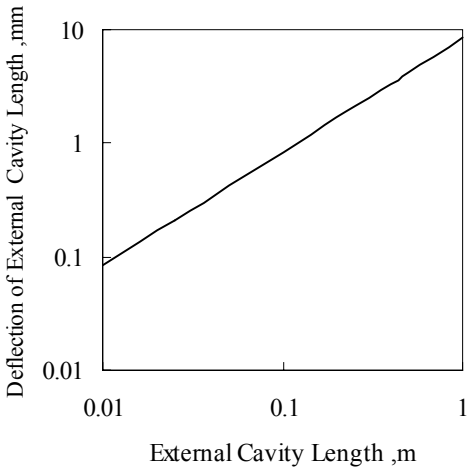

Figure 10. Relationship between External Cavity Length and Deflection External Cavity Length.

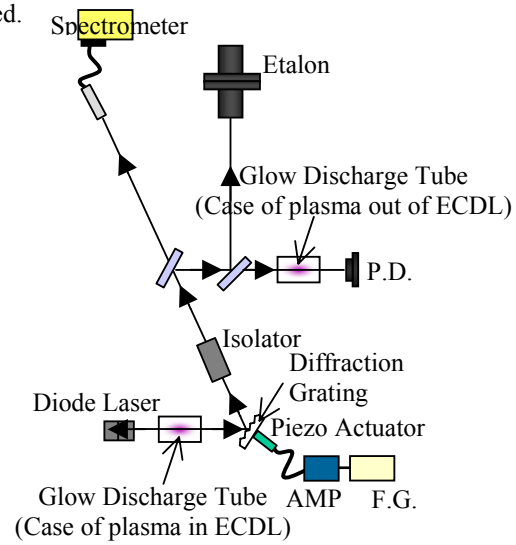

Figure 11. Schematic of measurement system for laser absorption usind the ECDL with a long cavity

B. Experimental Result

First, The relationship between injection current and optical power output with the Littrow-type external cavity is measured as shown in Fig. 12. From Fig.12 and Eqs. (12) (13), the parameters for this external cavity laser were estimated as shown in Table 3.

.

Table 3 Fitting parameters in diode laser

Measured Parameters		Fitting Parameters	
I_{th0}	Gradient	Γg_0	$<\alpha_i>/\alpha_m$
34.6mA	14.5mV	466cm^{-1}	83.8

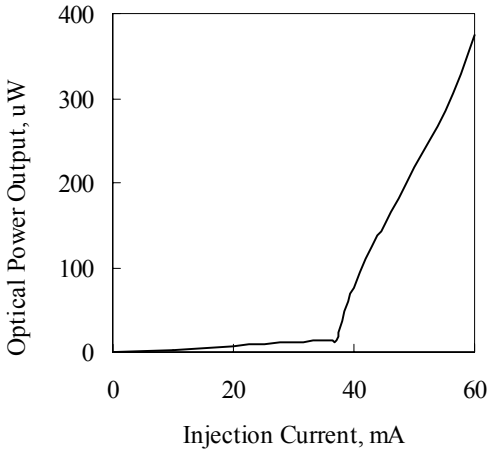

Figure 12. Measured Relationship between injection current and Optical Power Output

Next, Plasma is placed out of the ECDL. The absorption signal was measured as shown in Fig. 13. $(I_t/I_0)_{OUT}$ plotted by Gaussian fitting was obtained as shown in Fig. 14. The maximum absorbance for argon glow discharge was 0.42. From fitting parameters shown in Table 3, $(I_t/I_0)_{IN}$ was expected as shown in Fig 14 together.

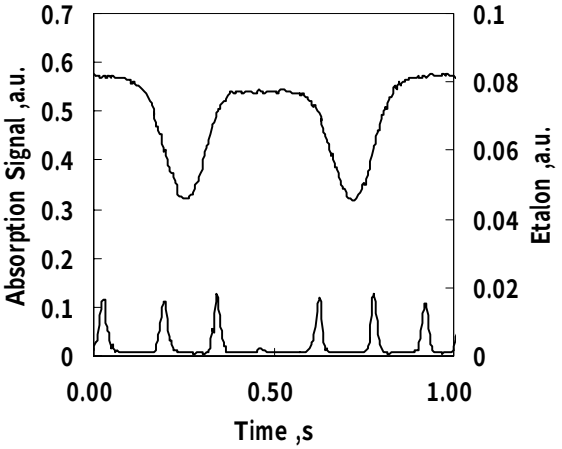

Figure 13. Absorption Signals by ECDL with Long Cavity Length

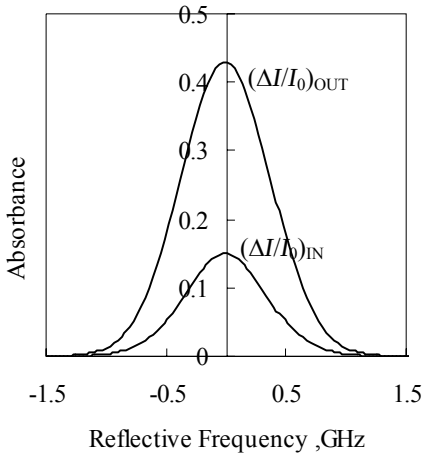

Figure 14. Measured $(\Delta I/I_0)_{OUT}$ by ECDL with Long Cavity Length and Calculated Prediction of $(\Delta I/I_0)_{IN}$.

Finally, the glow discharge tube is placed in ECDL as shown in Fig. 11. Absorption signal is shown in Fig. 15 and $(\Delta I/I_0)_{IN}$ was obtained as shown in Fig. 16.Maximum absorbance was smaller than that with plasma out of ECDL as calculated. The internal loss of this diode laser is large as shown in Table 3, $(\Delta I/I_0)_{IN}$ is lower than $(\Delta I/I_0)_{OUT}$. Therefore, using the diode laser where internal loss is low as discussed in Sec. III, sensitivity enhancement would be achieved.

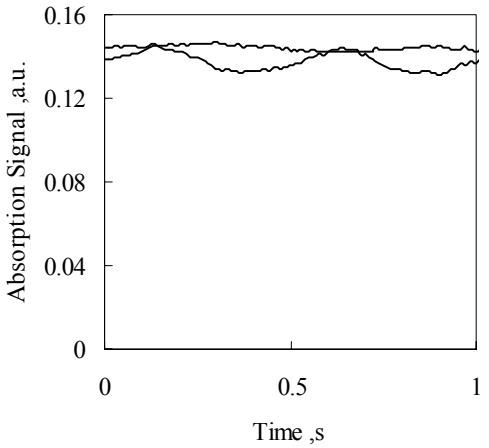

Figure 15. Experimental Result when plasma is place in ECDL

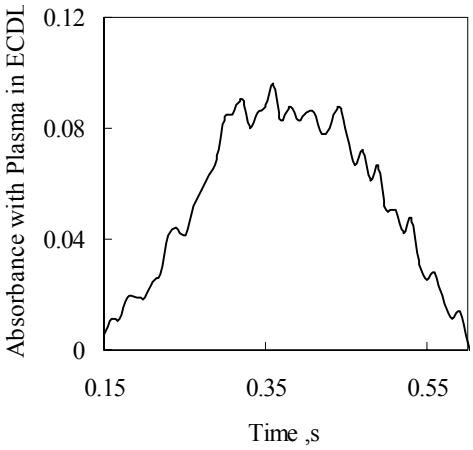

Figure 16. Absorbance with plasma in ECDL

V. Conclusion

1) A new multipass method of sensitivity enhancement for the laser absorption spectroscopy was developed and tested.
2) In the proposed method, the decrease of the injected current would cause the sensitivity enhancement and diode laser with low internal loss would be more effective.

VI. References

[1]Auweter-Kurtz, M., Kurtz, H. and Laure, S. "Plasma Generators for Re-Entry Simulation", Journal of Propulsion and Power, 1996, Vol. 12, No. 6 , pp.1053-1061.

[2]Matsui, M., Takayanagi, H., Oda, Y., Komurasaki, K., Arakawa, Y., "Performance of arcjet-type atomic-oxygen generator by laser absorption spectroscopy and CFD analysis", Vacuum, 2004, Vol.73, 3-4, pp.341-346

[3]Matsui, M., Komurasaki, K., and Arakawa, Y., "Laser Diagnostics of Atomic Oxygen in Arc-Heater Plumes", 40th AIAA Aerospace Science Meeting and Exhibit, AIAA 02-0793

[4]Auweter-Kurtz, M., G. Hedrich, S. Laure and H. Wagner, "Plasma sorce development for technical applications at IRS", VACUUM, 2004, Vol.73, pp.309-316

[5]Demtroder, W., "Laser Spectroscopy" Springer-Verlag, 1982

[6]Semen M. Chernin, Development of optical multipass matrix systems, Journal of modern optics, 2001, vol.48, No.4, pp.619-632

[7]Ralf Petry, Stefan Klee, Michael Lock, Brenda P. Winnewisser, and Manfred Winnewisser, Spherical mirror multipass system for FTIR jet spectroscopy: application to the rovibrationally resolved spectrum of $OC_5O^{\star}$, Journal of Molecular Structure, 2002, Vol.612, pp.369-381

[8]Larry A. Coldren and Scott W. Corzine, "Diode Lasers and Photonic Integrated Circuits," JOHN WILEY and SONS, INC., 1995

[9]F. J. Duarte, R. C. Sze, D. G. Harris, Charles Freed, Norman P. Barnes, Paul Zorabedian, and Stephen Vincent Benson, Tunable Lasers Handbook, 1995, Optics and Photonics